Eddy Viscosity and Velocity Distribution in Turbulent Pipe Flow Revisited

Ravindra Datta
Dept. of Chemical and Biochemical Engineering, The University of Iowa, Iowa City, IA 52242

An algebraic expression involving three universal constants is proposed for the eddy momentum diffusivity in fully developed turbulent pipe flow that adequately simulates its variation throughout the pipe cross-section. The model permits analytical integration to provide a single universal correlation that, unlike other available expressions, smoothly and accurately describes the entire turbulent velocity distribution from the inner region in the immediate vicinity of the wall all the way to the core region near the pipe axis and compares well with the existing correlations and experimental data. Accurate values of the maximum velocity and other flow variables of engineering interest can also be calculated from the velocity profile expression.

Introduction

The problem of fully developed turbulent flow in smooth pipes is of fundamental importance in many fields of engineering, and consequently a number of empirical or semiempirical correlations are available in the literature for describing the velocity and eddy viscosity distribution (Lin et al., 1953; Schlinger et al., 1953; Ranny, 1956; Corcoran et al., 1956; Spalding, 1961; Wasan et al., 1963; Brodkey, 1967; Hinze, 1975; Schlichting, 1979; Arpaci and Larsen, 1984; White, 1991). Typically, however, these models represent the experimental data only within their prescribed ranges of applicability or involve a great deal of empiricism (for example, Brodkey, 1963; Pai, 1953). A satisfactory *single* correlation, with a minimum of fitted parameters, that smoothly represents the entire distribution from the viscous sublayer in the immediate vicinity of the pipe wall to the core region, has so far proved to be elusive (Brodkey, 1967). This work tries to provide such a correlation.

Although variations of the theme exist, it is customary to divide the entire flow cross-section into: *i*) an inner or near-wall region; *ii*) an outer or core region; and *iii*) an overlap region, in the spirit of the technique of singular perturbation, now invoked to obtain the logarithmic law in the overlap region, which was derived originally by other less rigorous arguments. In the wall region, by dimensional considerations, then

$$U^+ = \phi(y^+) \tag{1}$$

otherwise known as the *law of the wall*. In the outer region ($0.15\text{-}0.2 \le y/R \le 1.0$), on the other hand, the data are generally correlated by the so-called *velocity defect law*:

$$U^+_{max} - U^+ = \psi(1-\xi) \tag{2}$$

which is in terms of the dimensionless radial distance, $\xi \equiv r/R$, that is $\sim O(1)$, whereas the small distances in the inner region are stretched by scaling with the length scale, ν/U^*, which is $\sim O(0)$. In the overlap layer, the gradients of the inner and outer solutions, Eqs. 1 and 2 are matched (Kundu, 1990, p. 452), resulting in the *logarithmic law*:

$$U^+ = \frac{1}{\kappa} \ln y^+ + A \tag{3}$$

which is valid in the region $30\text{-}50 \le y^+ < 0.2y_0^+$. The constants in this equation, namely, κ (von Kármán constant) and A, are presumably universal. The most popular values, based on the experiments of Nikuradse (Schlichting, 1979), are $A = 5.5$ and $\kappa = 0.4$, although many other sets of values have been proposed by other investigators, varying in the range $\kappa = 0.36$ to 0.419 and $A = 3.8$ to 5.85 (Deissler, 1955; Patel, 1965; Hinze, 1975; Arpaci and Larsen, 1984; White, 1991). The wall region is usually further subdivided into a composite of two quite thin layers—a viscous sublayer adjacent to the wall, and a buffer layer between the overlap layer and the viscous sublayer. Thus, $\phi(y^+)$, Eq. 1, usually comprises two expressions:

Viscous sublayer ($0 \le y^+ < 5-8$), where

$$U^+ = y^+ \tag{4}$$

and buffer layer ($5\text{-}8 \le y^+ < 30-50$), where

$$U^+ = 5.0 \ln y^+ - 3.05 \tag{5}$$

An alternative single expression for the wall region is given by Spalding (1961), which is of the form, $y^+ = f(U^+)$, rather than of the type $U^+ = \phi(y^+)$.

In pipe flow, the wake is only slight, and consequently the deviations from Eq. 3 in the core region are rather small. It is, therefore, assumed to be applicable all the way to the pipe axis. Thus, the so-called "universal velocity distribution," given by the patchwork of Eqs. 3 to 5 adequately describes the fully turbulent velocity profile in pipes (for $N_{Re} \ge 30{,}000$), even though it possesses some undesirable features, as discussed by Brodkey (1967).

Theoretical Model

Momentum balance

Momentum balance for fully developed pipe flow gives:

$$\tau_{rz} = \rho (U^*)^2 \xi \tag{6}$$

where the total stress, $\tau_{rz} = -\mu dU/dr + \rho(\overline{v'u'})$. Utilizing the hypothesis of Boussinesq for the Reynolds stress, $\rho(\overline{v'u'}) \equiv -\rho\epsilon dU/dr$:

$$\tau_{rz} = -\mu(1+\epsilon_r)\frac{dU}{dr} \tag{7}$$

Equations 6 and 7 are equated and written in the dimensionless form:

$$-(1+\epsilon_r)\frac{dU^+}{d\xi} = \frac{N_{vK}}{2\sqrt{2}}\xi \tag{8}$$

where the von Kármán number, $N_{vK} \equiv N_{Re}\sqrt{f}$. Equation 8 can be integrated to obtain the velocity profile, provided a model for ϵ_r is available. This is developed next.

Eddy momentum diffusivity model

To construct a robust model for the eddy momentum diffusivity, the different variables that could possibly affect ϵ are first enumerated (Deissler, 1955):

$$\epsilon = \epsilon\left(U, \nu, \rho, \tau_w, d_0, y, e, \frac{dU}{dy}, \frac{d^2U}{dy^2}, \ldots\right) \tag{9}$$

Various investigators have correlated ϵ in terms of one or more of these variables. For instance, Prandtl's mixing-length model (Brodkey, 1967; Hinze, 1975) assumes $\epsilon = \epsilon(y, dU/dy)$; von Kármán's similarity hypothesis supposes $\epsilon = \epsilon(dU/dy, d^2U/dy^2)$; Rannie (1956) has assumed $\epsilon = \epsilon(y, \tau_w, \rho, \nu)$; Deissler (1955) assumes $\epsilon = \epsilon(U, y, \nu)$; Schlinger et al. (1953), Reichardt (as cited by Arpaci and Larsen, 1984), as well as Reynolds et al. (as cited by Wilson and Azad, 1975) assume $\epsilon = \epsilon(y, d_0, \tau_w, \rho, \nu)$; and Spalding (1961) assumes $\epsilon = \epsilon(U, \tau_w, \rho)$. Here, the following form is adopted:

$$\epsilon = \epsilon(U, \nu, \rho, \tau_w, d_0) \tag{10}$$

in which any dependence on the velocity gradients is neglected and it is assumed that any y dependence is implicitly included in U. The effect of wall roughness, e, is also neglected since we are here concerned only with smooth pipes. Dimensional analysis then yields:

$$\epsilon_r = \epsilon_r(U^+, N_{vK}) \tag{11}$$

To develop an algebraic expression for ϵ_r in terms of U^+ and N_{vK}, let us next consider the salient traits that a suitable expression must possess:

1. At the wall, where $y = 0$, $U^+ = 0$, and $\epsilon_r = 0$.
2. In the immediate vicinity of the wall, as $y^+ \to 0$, Elrod (1957) has shown that, since the turbulence velocity components have to satisfy the equation of continuity, $\epsilon_r \propto (y^+)^4$ for an incompressible fluid. Since in this region, $U^+ = y^+$, an appropriate expression must conform to $\epsilon_r \propto (U^+)^4$.
3. ϵ_r increases essentially linearly with y beyond the buffer layer and throughout the overlap layer (Hinze, 1975, pp. 621, 645).
4. There is a maximum in ϵ_r roughly midway between the wall and the pipe axis and it then decreases toward the pipe axis (Schlichting, 1979, p. 609).
5. ϵ_r approaches a finite value at the pipe axis. However, there is little concensus on the numerical value of ϵ_r at the pipe axis (Schlichting, 1979, p. 609; Hinze, 1975, p. 730), which likely also depends on the Reynolds number.

Based on above, the following specific form for ϵ_r in Eq. 11 is suggested:

$$\epsilon_r = \sinh^4\left(\frac{U^+}{\alpha}\right)\left\{1 - \frac{\sinh\left(\frac{\beta U^+}{\alpha}\right)}{\sinh\left(\frac{\delta\beta U^+_{\max}}{\alpha}\right)}\right\} \tag{12}$$

where $U^+_{\max} = U^+_{\max}(N_{vK})$, as discussed later. Equation 12 includes three constants: α, β, and δ. In comparison, the universal velocity profile given by Eqs. 3 to 5 involves four fitted constants, while the more recent $k-\bar{\epsilon}$ formulation involves many more parameters (Patel et al., 1985). Another distinct advantage of the proposed model is that it permits analytical determination of the velocity and other quantities of interest.

It is evident that the first term in Eq. 12 satisfies the requirements 1 and 2 listed above. The fourth power of the sinh function ensures that $\epsilon_r \to (U^+/\alpha)^4$ as $y^+ \to 0$, as can be seen from the Taylor series expansion of the first term. The constant α, therefore, can be determined from the variation of ϵ_r in the neighborhood of the wall. The form of the term in the braces in Eq. 12 was chosen to emulate the variation of ϵ_r in the overlap layer and the outer region as described by requirements 3 to 5 above. The choice of the values of β and δ determines the numerical value and location of the maximum in ϵ_r as well as its value at the pipe axis. Thus, δ is expected to be only slightly higher than unity. Indeed, if $\delta = 1.0$, Eq. 12 yields $\epsilon_r = 0$ at the pipe axis.

Velocity distribution

The velocity profile is obtained by separating the variables

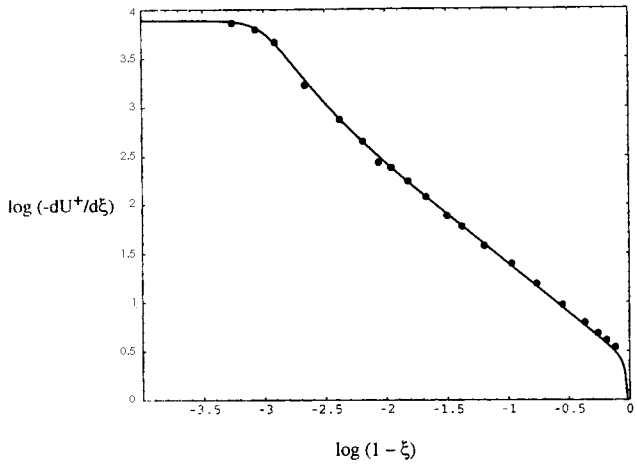

Figure 1. Variation of the log($-dU^+/d\xi$) vs. log(1 − ξ).

Comparison of theory, Eq. 13 and its derivative, with velocity gradient data calculated from mean velocity profile data of Patel (1965).

and integrating Eq. 8 while using the boundary condition at the wall. This yields the implicit expression:

$$U^+ + \alpha F(U^+) = \frac{N_{vK}}{4\sqrt{2}}(1-\xi^2) \tag{13}$$

where the function

$$F(U^+) \equiv \int_0^{U^+/\alpha} \epsilon_r(x)dx \tag{14}$$

where x is a dummy variable for (U^+/α). Using the model for ϵ_r given by Eq. 12 in Eq. 14 results in:

$$\begin{aligned} F(U^+) = &\left\{\frac{\gamma}{\beta(\beta^2-16)(\beta^2-4)}\right\}\cdot\left[24-\frac{1}{8}\cosh\left(\beta\frac{U^+}{\alpha}\right)\right. \\ &\left.\cdot\left\{192-60\beta^2+3\beta^4-4\beta^2(\beta^2-16)\cosh\left(2\frac{U^+}{\alpha}\right)\right\}\right] \\ &+\left\{\frac{\gamma\beta}{8(\beta^2-16)}\right\}\left\{\cosh\left(\beta\frac{U^+}{\alpha}\right)\cosh\left(4\frac{U^+}{\alpha}\right)\right\} \\ &+\frac{1}{32}\left\{12\frac{U^+}{\alpha}-8\sinh\left(2\frac{U^+}{\alpha}\right)+\sinh\left(4\frac{U^+}{\alpha}\right)\right\} \\ &+\left\{\frac{\gamma}{(\beta^2-16)(\beta^2-4)}\right\}\left\{\sinh\left(2\frac{U^+}{\alpha}\right)\sinh\left(\beta\frac{U^+}{\alpha}\right)\right\} \\ &\cdot\left\{16-\beta^2-4\cosh\left(2\frac{U^+}{\alpha}\right)+\beta^2\cosh\left(2\frac{U^+}{\alpha}\right)\right\} \end{aligned} \tag{15}$$

where the parameter γ is defined by:

$$\gamma \equiv \frac{1}{\sinh\left(\frac{\delta\beta U^+_{\max}}{\alpha}\right)} \tag{16}$$

and is a function of N_{vK} only. It may be noted that for meaningful results $\beta > 4.0$. Thus, Eq. 13, along with Eq. 15, implicitly provides the variation of the velocity with the dimensionless radial distance, ξ, for the fully developed turbulent flow. This form is suitable for the velocity distribution in the outer region. However, the wall coordinate, y^+, is more appropriate for the inner region, which is related to ξ by:

$$y^+ = \frac{N_{vK}}{2\sqrt{2}}(1-\xi) \tag{17}$$

Using this in Eq. 13 gives:

$$y^+ = \frac{N_{vK}}{2\sqrt{2}}\left\{1-\sqrt{1-\frac{4\sqrt{2}}{N_{vK}}[U^+ + \alpha F(U^+)]}\right\} \tag{18}$$

where $F(U^+)$ is given by Eq. 15. Equation 18, like the expression of Spalding (1961), is of the form $y^+ = f(U^+)$, rather than *vice versa*, as is customary but, of course, presents little difficulty in the calculation of velocity distribution.

Results and Discussion

Although data on pipe flow have been reported by many over a period of more than half a century, there is a considerable variation among the results of different investigators. Here, we use the relatively more recent velocity profile data given by Patel (1965) for comparison. See also Patel and Head (1969).

Equations 12 and 16 require the value of $U^+_{\max} = U^+_{\max}(N_{vK})$. This is determined by setting $\xi = 0$, and $U^+ = U^+_{\max}$ in Eq. 13, that is, by solving:

$$U^+_{\max} + \alpha F(U^+_{\max}) = \frac{N_{vK}}{4\sqrt{2}} \tag{19}$$

where the function F is given by Eq. 15. The values of the three constants used in all of the calculations here are: $\alpha = 10.25$, $\beta = 4.17$, and $\delta = 1.008$. While these values, of course, are not sacrosanct, they are believed to be "universal" to the same extent as are the constants of the logarithmic law. Since calculation of $U^+_{\max}$ from Eq. 19 requires root finding of an algebraically involved expression, it may alternatively be estimated from the following explicit expression of the form of Eq. 3, with $y^+ = y_0^+ = N_{vK}/2\sqrt{2}$, from Eq. 17, and a slight adjustment of the constants:

$$U^+_{\max} \approx 2.505 \ln\left(\frac{N_{vK}}{2\sqrt{2}}\right) + 5.06 \tag{20}$$

Eddy viscosity

Eddy viscosity distribution was calculated from the mean velocity profile data of Patel (1965) using Eq. 8, which involves differentiation of the velocity data to obtain the velocity gradient. These data are for $N_{vK} = 21{,}850$, calculated from the plotted value of y_0^+ (Patel, 1965), which corresponds to a $N_{Re} \approx 370{,}000$. The velocity gradient was calculated first by curve-fitting the velocity distribution data in the different regions followed by analytical differentiation of the fitted equations. The results are shown in Figure 1 along with the theoretical prediction obtained by differentiating Eq. 13, which

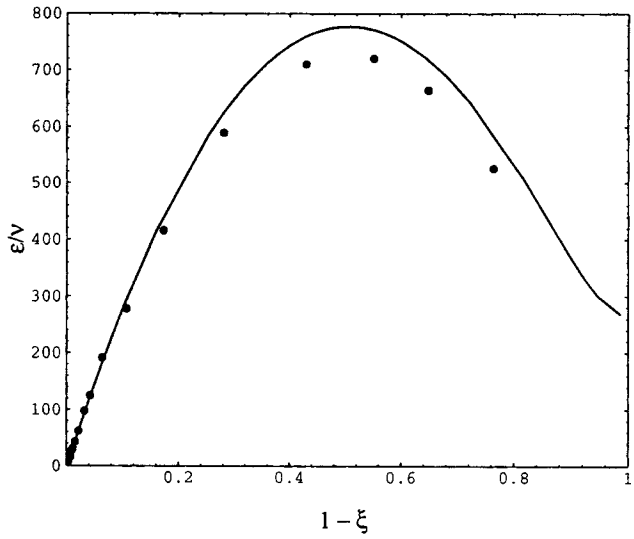

Figure 2. Distribution of relative eddy momentum diffusivity.

Comparison of values calculated from mean velocity profile data of Patel (1965) with Eq. 12.

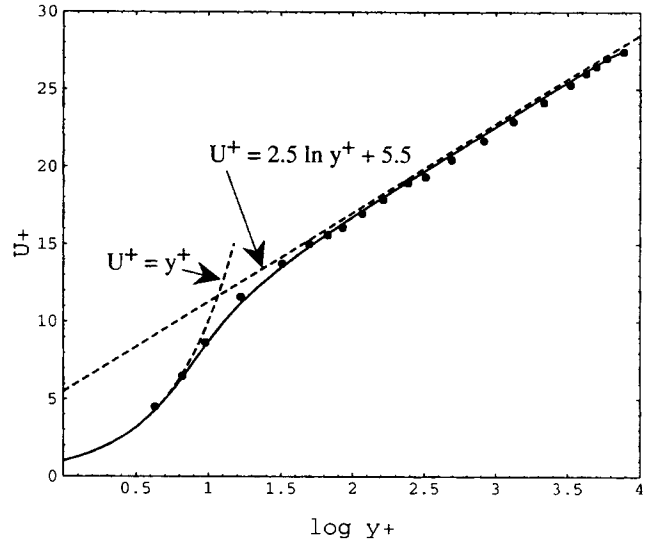

Figure 4. Mean velocity profile in the universal coordinates.

Comparison of Eq. 18 with the data of Patel (1965), and the universal velocity profile, Eqs. 3 and 4.

provides $dU^+/d\xi$ for a given U^+, while the corresponding ξ is calculated from Eq. 13. It is seen that the agreement is quite good throughout the flow cross-section.

Figure 2 shows a comparison of Eq. 12 with the relative eddy viscosity values calculated from the data of Patel (1965) as described above. Note that the maximum value of ϵ is ~ 720 times ν for this N_{vK}! The expression agrees reasonably well with the calculated values throughout the pipe cross-section and has a maximum error of 7%. The agreement is actually much better in the inner region than in the outer region, where the error in calculating ϵ_r is also the largest. It is noteworthy, however, that Eq. 12 predicts the gross features in the outer region quite well including the maximum and a finite value of ϵ_r at the pipe axis. The variation of ϵ_r in the wall region is shown in Figure 3. Also plotted in this figure is the limiting form of Eq. 12 close to the wall where $U^+ \ll U^+_{\max}$ and consequently Eq. 12 reduces to:

$$\epsilon_r \approx \sinh^4\left(\frac{U^+}{\alpha}\right) \tag{21}$$

The agreement of both expressions is quite good in the range of y shown. Therefore, the simpler expression for ϵ_r, Eq. 21, that involves a *single* fitted constant α provides results of acceptable accuracy in the wall and the overlap regions. Although not shown here, similar calculations of ϵ_r distribution were also made for the experimental conditions of Nikuradse ($N_{Re} = 1.1 \times 10^5$ to 3.2×10^6) and agreed reasonably well with the corresponding results given by Schlichting (1979, p. 609).

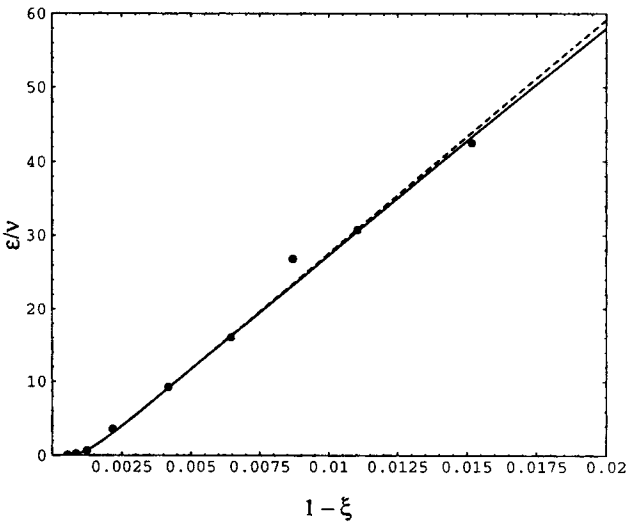

Figure 3. Variation of relative eddy momentum diffusivity in the wall region.

Comparison of Eq. 12 and its asymptotic form, Eq. 21 (broken line), with data calculated from mean velocity profile data of Patel (1965).

Velocity distribution

Figure 4 shows the mean velocity profile data of Patel (1965) in the usual universal coordinates, namely U^+ vs. $\log y^+$. The agreement of Eq. 18 with the data is excellent up to $y^+ \approx 300$ and also from $y^+ \approx 2{,}500$ to the pipe axis ($y_0^+ = 7{,}725$). However, there is a slight deviation in the intermediate range. Overall, the agreement is considered to be quite good, including an accurate prediction of $U^+_{\max}$. It is seen that Eq. 18 also agrees quite well with the usual limiting expressions of the universal velocity distribution, Eqs. 3 and 4. While not shown here, the model predictions also compared favorably with the velocity profile data of Nikuradse (Schlichting, 1979, p. 601). Figure 5 compares the velocity distribution data with Eq. 13 in a linear form of $U/U_{\max}$ vs. $(1-\xi)$. A closer inspection of the region adjacent to the wall in the inset of Figure 5 also shows excellent agreement. Finally, the velocity profile is plotted in Figure 6 in the velocity defect form of Eq. 2.

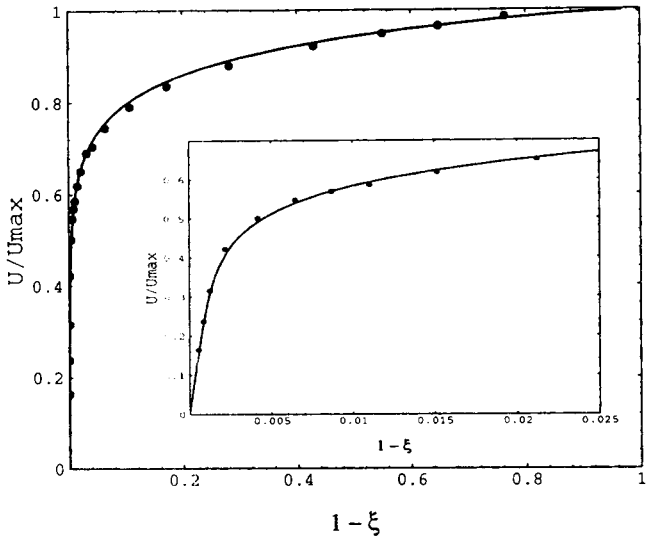

Figure 5. Mean velocity as a ratio of the maximum velocity vs. dimensionless distance from wall.

Comparison of Eq. 13 with the data of Patel (1965).

Acknowledgment

I am pleased to acknowledge the helpful suggestions and comments of Professor V. C. Patel, Iowa Institute of Hydraulic Research, The University of Iowa.

Notation

A = constant in logarithmic law, Eq. 3
d_0 = pipe inner diameter
e = wall roughness factor
f = Fanning friction factor = $\tau_w/(1/2)\rho U_{ave}^2$
$F(U^+)$ = function defined by Eq. 14 and given by Eq. 15
k = turbulent kinetic energy
ℓ = mixing length
N_{Re} = Reynolds number = $d_0 U_{ave}/\nu$
N_{vK} = von Karman number = $N_{Re}\sqrt{f} = \sqrt{2}\, d_0 U^*/\nu$

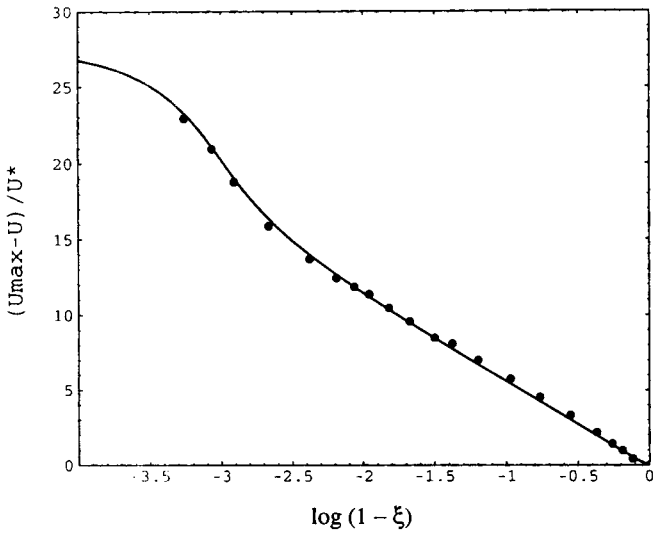

Figure 6. Mean velocity defect profile.

Comparison of Eq. 13 with the data of Patel (1965).

r = radial coordinate
R = pipe inner radius
u' = turbulent velocity fluctuation in axial direction
U = time mean axial velocity
U^* = friction velocity = $\sqrt{\tau_w/\rho}$
U^+ = dimensionless axial velocity = U/U^*
U_{ave} = cross-sectional area average velocity
U^+_{ave} = dimensionless area average velocity = U_{ave}/U^*
U_{max} = maximum (centerline) velocity
U^+_{max} = dimensionless maximum (centerline) velocity = U_{max}/U^*
v' = turbulent velocity fluctuation in radial direction
x = dummy variable for (U^+/α) in Eq. 14
y = normal distance from the pipe wall = $R - r$
y^+ = dimensionless normal distance from the pipe wall = yU^*/ν
y_0^+ = maximum dimensionless normal distance from wall = $RU^*/\nu = N_{vK}/2\sqrt{2}$
z = axial coordinate

Greek letters

α = universal constant in eddy diffusivity model, Eq. 12 = 10.25
β = universal constant in eddy diffusivity model, Eq. 12 = 4.17
γ = parameter defined by Eq. 16 = $1/\sinh[\delta\beta U^+_{max}/\alpha]$
δ = universal constant in eddy diffusivity model, Eq. 12 = 1.008
ϵ = eddy momentum diffusivity
ϵ_r = relative eddy momentum diffusivity = ϵ/ν
$\bar{\epsilon}$ = rate of dissipation of the turbulent kinetic energy
κ = von Karman constant in logarithmic law, Eq. 3
μ = fluid viscosity
ν = fluid kinematic viscosity = μ/ρ
ξ = dimensionless radial distance = r/R
ρ = fluid density
τ_{rz} = shear stress
τ_w = shear stress at the wall
ϕ = law of the wall, Eq. 1
ψ = velocity defect law, Eq. 2

Literature Cited

Arpaci, V. S., and P. S. Larsen, *Convection Heat Transfer*, Prentice-Hall, Englewood Cliffs, NJ (1984).

Brodkey, R. S., "Limitations on a Generalized Velocity Distribution," *AIChE J.*, **9**, 448 (1963).

Brodkey, R. S., *The Phenomena of Fluid Motions*, Addison-Wesley, Reading, MA (1967).

Corcoran, W. H., J. B. Opfell, and B. H. Sage, *Momentum Transfer in Fluids*, Academic Press, New York (1956).

Deissler, R. G., "Analysis of Turbulent Heat Transfer, Mass Transfer and Friction in Smooth Tubes at High Prandtl and Schmidt Numbers," *NACA Report 1210*, 69 (1955).

Elrod, Jr., H. G., "Note on Turbulent Shear Stresses Near a Wall," *J. Aeronaut. Sci.*, **24**, 468 (1957).

Hinze, J. O., *Turbulence*, 2nd ed., McGraw-Hill, New York (1975).

Kundu, P. K., *Fluid Mechanics*, Academic Press, New York (1990).

Lin, C. S., R. W. Moulton, and G. L. Putnam, "Mass Transfer between Solid Wall and Fluid Stream," *Ind. Eng. Chem.*, **45**, 636 (1953).

Pai, S. I., "On Turbulent Flow Between Parallel Plates," *J. Appl. Mech.*, **20**, 109 (1953).

Patel, V. C., "Calibration of the Preston Tube and Limitations on its Use in Pressure Gradients," *J. Fluid Mech.*, **23**, 185 (1965).

Patel, V. C., and M. R. Head, "Some Observations on Skin Friction and Velocity Profiles in Fully Developed Pipe and Channel Flows," *J. Fluid Mech.*, **38**, 181 (1969).

Patel, V. C., W. Rodi, and G. Scheuerer, "Turbulence Models for Near-Wall and Low Reynolds Number Flows: A Review," *AIAA J.*, **23**, 1308 (1985).

Rannie, W. D., "Heat Transfer in Turbulent Shear Flow," *J. Aeronaut. Sci.*, **23**, 485 (1956).

Schlichting, H., *Boundary-Layer Theory*, 7th ed., McGraw-Hill, New York (1979).
Schlinger, W. G., V. J. Berry, J. L. Mason, and B. H. Sage, "Temperature Gradients in Turbulent Gas Streams," *Ind. Eng. Chem.*, **45**, 662 (1953).
Spalding, D. B., "A Single Formula for the 'Law of the Wall'," *Trans. ASME, J. Appl. Mech.*, **28E**, 455 (1961).
Wasan, D. T., C. L. Tien, and C. R. Wilke, "Theoretical Correlation of Velocity and Eddy Viscosity for Flow Close to a Pipe Wall," *AIChE J.*, **9**, 567 (1963).
White, F. M., *Viscous Fluid Flow*, 2nd ed., McGraw-Hill, New York (1991).
Wilson, N. W., and R. S. Azad, "A Continuous Prediction Method for Fully Developed Laminar, Transitional, and Turbulent Flow in Pipes," *J. Appl. Mech.*, **42**, 51 (1975).

Manuscript received July 13, 1992, and revision received Dec. 18, 1992.